

## Parametric modeling and shape optimization of four typical Schwedler spherical reticulated shells

J. Wu<sup>1,2a</sup>, X.Y. Lu<sup>2b</sup>, S.C. Li<sup>1c</sup>, Z.H. Xu<sup>\*1</sup>, L.P. Li<sup>1d</sup>, D.L. Zhang<sup>3e</sup> and Y.G. Xue<sup>1f</sup>

<sup>1</sup>Geotechnical and Structural Engineering Research Center, Shandong University,  
Ji'nan 250061, Shandong, China

<sup>2</sup>Institute of Engineering Mechanics, Shandong Jianzhu University, Ji'nan 250101, Shandong, China

<sup>3</sup>Shandong Agriculture and Engineering University, Ji'nan 250100, Shandong, China

(Received December 5, 2014, Revised November 2, 2015, Accepted November 9, 2015)

**Abstract.** Spherical reticulated shells are widely applied in structural engineering due to their good bearing capability and attractive appearance. Parametric modeling of spherical reticulated shells is the basis of internal analysis and optimization design. In the present study, generation methods of nodes and the corresponding connection methods of rod elements are proposed. Modeling programs are compiled by adopting the ANSYS Parametric Design Language (APDL). A shape optimization method based on the two-stage algorithm is presented, and the corresponding optimization program is compiled in FORTRAN environment. Shape optimization is carried out based on the objective function of the minimum total steel consumption and the restriction condition of strength, stiffness, slenderness ratio, stability. The shape optimization of four typical Schwedler spherical reticulated shells is calculated with the span of 30 m~80 m and rise to span ratio of 1/7~1/2. Compared with the shape optimization results, the variation rules of total steel consumption along with the span and rise to span ratio are discussed. The results show that: (1) The left and right rod-Swedler spherical reticulated shell is the most optimized and should be preferentially adopted in structural engineering. (2) The left diagonal rod-Swedler spherical reticulated shell is second only to left and right rod regarding the mechanical behavior and optimized results. It can be applied to medium and small-span structures. (3) Double slash rod-Swedler spherical reticulated shell is advantageous in mechanical behavior but with the largest total weight. Thus, this type can be used in large-span structures as far as possible. (4) The mechanical performance of no latitudinal rod-Swedler spherical reticulated shell is the worst and with the second largest weight. Thus, this spherical reticulated shell should not be adopted generally in engineering.

**Keywords:** schwedler spherical reticulated shell; APDL; parametric modeling; shape optimization

---

\*Corresponding author, Lecturer, E-mail: zhenhao\_xu@sdu.edu.cn

<sup>a</sup>Ph.D. Student, E-mail: wujing9516@163.com

<sup>b</sup>Professor, E-mail: luxy5504@163.com

<sup>c</sup>Professor, E-mail: lishucai@sdu.edu.cn

<sup>d</sup>Associate Professor, E-mail: yuliyangfan@163.com

<sup>e</sup>M. Eng., E-mail: daliang08@sina.com

<sup>f</sup>Professor, E-mail: xieagle@sdu.edu.cn



(a) National Stadium of Australia

(b) National Theatre of China

Fig. 1 Examples of reticulated shell structures

## 1. Introduction

In recent years, spherical reticulated shells have been used widely in domestic and foreign public buildings due to the advantages of rod-system and thin-shell, i.e., good appearance, reasonable stress and large stiffness (Shen and Chen 1996). They have vast application prospects in modern large-span building structures (Dong and Yao 2003), such as major sports/arts venues, waiting halls and shopping malls (Fig. 1). However, the number of nodes and rod elements of spherical reticulated shells are too many and the variation of span, height, grid size, type and other parameters can cause structural internal force reallocation. The workload of re-modeling is very large and it is quite difficult to carry out high efficient stress analysis and structural optimization design. In addition, structural materials of spherical reticulated shells are ideal but of high cost. Thus, shape optimization is quite necessary and important for the design and construction of spherical reticulated shells.

Schwedler spherical reticulated shells are typical and widely used structures in modern architectural reticulated shells because they are easy to calculate and install. In addition, they have advantages of small number of nodes and light weight, etc. Conventional modeling of these structures often relies on hand-modeling rather than on parametric modeling in domestic and foreign studies. Relevant research is also seldom related to the specific work of shape optimization design.

At present, continuous variable optimization is now well-established, but the research on optimum design of discrete variables is not many. Now the main research results are as follows: Lipson and Gwin (1977) researched discrete sizing of trusses for optimal geometry. The optimal configuration and discrete member sizes were automatically determined to minimize the cost of three-dimensional indeterminate truss structures under multiple loading conditions. Member areas and joint coordinates were used as design variables. Svanberg (1987) presented a new method for non-linear programming in general and structural optimization in particular. In each step of the iterative process, a strictly convex approximating sub problem was generated and solved. Jenkins studied structural optimization with the genetic algorithm (1991) and natural algorithm (1997). Salajegheh and Vanderplaats (1993) presented a method for optimizing truss structures with discrete design variables, and the design variables were considered to be sizing variables as well as

coordinates of joints. Moreover, both types of variables could be discrete simultaneously and mixed continuous-discrete variables could also be considered. Rajan (1995) developed a procedure for the combined sizing, shape, and topology design of space trusses. Sun *et al.* (1995) proposed a two-level algorithm for shape optimization of space trusses with discrete sizing variables. Chai and Sun (1996) presented a two-level combination algorithm for solving (0, 1, 2) planning issues. Saka and Kameshki (1998) investigated optimum design of nonlinear elastic framed domes, i.e., an algorithm was presented for the optimum design of three-dimensional rigidly jointed frames which took into account the nonlinear response due to the effect of axial forces in members. Salajegheh (2000) achieved optimum design of structures with multiple frequency constraints, and a two-point approximation was employed to approximate the frequency. Xu *et al.* (2006) investigated an optimal method, and this optimum design was performed by the combination of the direct searching method and the criterion. Vyzantiadou *et al.* (2007) proposed structural systems. The proposed computational method produces algorithms using fractal mathematics, and could generate forms applicable to shells. Yas *et al.* (2007) introduced the stacking sequence optimization of a laminated cylindrical shell for obtaining maximum natural frequency and buckling stress, simultaneously. Rahami *et al.* (2008) developed a combination of energy and force method, and genetic algorithm was employed as an optimization tool for minimizing the weight of the truss structures. Dietl and Garcia (2010) proposed a new approach to change the shape of the beam to concentrate the strain in sections of the beam where it can contribute the most to transduction. Wu *et al.* (2010) investigated a new design concept of MAS, and a shape optimization method with finite element analysis was applied on two-dimensional (2D) stent models. Fraternali *et al.* (2011) employed the variation AL theory of optimal control problems and evolutionary algorithms to investigate the form finding of minimum compliance elastic structures. Durgun and Yildiz (2012) introduced a new optimization algorithm, called the Cuckoo Search Algorithm algorithm, for solving structural design optimization problems. The CS algorithm was applied to the structural design optimization of a vehicle component to illustrate how the present approach can be applied for solving structural design problems. Xia *et al.* (2012) presented a level set solution to the stress-based structural shape and topology optimization. A novel global measure of stress was proposed, and the optimization problem was formulated to minimize the global measure of stress subject to a constraint of material volume. Luo *et al.* (2012) also studied a meshless Galerkin level set method for shape and topology optimization of continuum structures. Gholizadeh and Barzegar (2013) proposed an efficient harmony search based algorithm for solving the shape optimization problem of pin-jointed structures subject to multiple natural frequency constraints. Yildiz (2013) investigated a comparison of evolutionary-based optimization techniques for structural design optimization problems. Furthermore, a hybrid optimization technique based on differential evolution algorithm was introduced for structural design optimization problems. Emmanuel *et al.* (2014) used ANN and GA for buckling optimization of laminated composite plate with elliptical cutout. In addition, the publications (Chiu 2010, Pedersen 2010, Qian 2010, Kaveh and Ahmadi 2014, Kaveh and Zolghadr 2014) also considered the structural optimization design.

The present study firstly describes main geometric parameters of spherical reticulated shells in section 2. Generation methods of nodes and connection methods of rod elements are proposed, and the corresponding modeling programs are compiled by adopting the ANSYS Parametric Design Language (APDL) in section 3. The proposed modeling method is simple, efficient and practical, which can provide the possibility for quickly generating different types of Schwedler reticulated spherical shells. Then, the selection of rod element types is introduced in section 4. The internal forces of four typical Schwedler spherical reticulated shells are analyzed and discussed in section

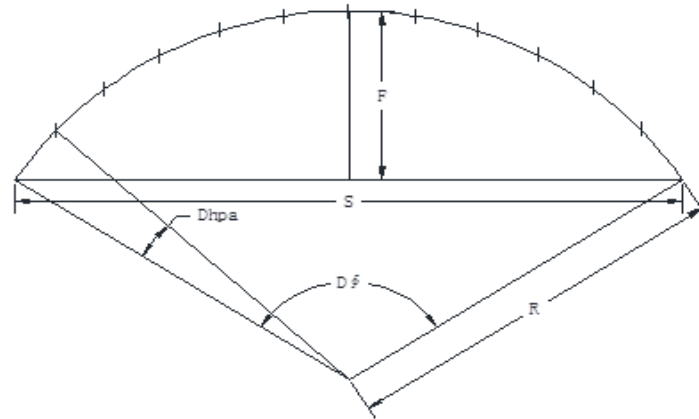


Fig. 2 Geometric schematic diagram of spherical reticulated shells

5. A shape optimization method based on the two-stage algorithm is presented in section 6, and the corresponding optimization program is compiled in FORTRAN environment. Thus, the total steel consumption of Schwedler spherical reticulated shells is optimized to be the lightest and the production costs are also optimized to be the least. The shape optimization of four typical Schwedler spherical reticulated shells are carried out with the span of 30 m~80 m and rise to span ratio of 1/7~1/2. Finally, compared with the shape optimization results, the variation rules of the total steel consumption along with the span and rise to span ratio are analyzed and discussed in section 7. The analysis results have some guiding significance for engineering design of Schwedler spherical reticulated shells (Wu 2013).

## 2. Geometric definitions

The shell span ( $S$ ), rise ( $F$ ), latitudinal portions ( $Kn$ ) and radial loops ( $Nx$ ) are main geometric parameters of describing spherical reticulated shells, which is shown in Fig. 2. The curvature radius of sphere  $R$  and global angle  $Dpha$  of two radial neighboring circle nodes are expressed by Eqs. (1)-(2) (Shen and Chen 1996). The derivation process of Eq. (2) is also given in detail.

$$R = \frac{\frac{S^2}{4} + F^2}{2F} \quad (1)$$

$$Dpha = \begin{cases} \frac{1}{Nx} \arctan\left(\frac{S}{2} / \sqrt{R^2 - \left(\frac{S}{2}\right)^2}\right) & \frac{F}{S} \neq \frac{1}{2} \\ \frac{90}{Nx} & \frac{F}{S} = \frac{1}{2} \end{cases} \quad (2)$$

As for Eq. (2), firstly, the total global angle  $D\phi$ ,  $\tan \frac{D\phi}{2} = \frac{S}{2} / \sqrt{R^2 - \left(\frac{S}{2}\right)^2}$

then,  $D\phi = 2 \arctan\left(\frac{S}{2} / \sqrt{R^2 - \left(\frac{S}{2}\right)^2}\right)$ , finally, the global angle  $Dpha$  of two radial neighboring circle nodes is calculated, i.e.,

$$Dpha = \frac{2\arctan\left(\frac{S}{2} / \sqrt{R^2 - \left(\frac{S}{2}\right)^2}\right)}{2N_x} = \frac{\arctan\left(\frac{S}{2} / \sqrt{R^2 - \left(\frac{S}{2}\right)^2}\right)}{N_x}$$

### 3. Parametric models of four typical Schwedler spherical reticulated shells

In the spherical coordinates given the shell span ( $S$ ), rise ( $F$ ), latitudinal portions ( $Kn$ ), radial loops ( $N_x$ ), then radius of curvature  $R$  and global angle  $Dpha$  are calculated. The nodes are generated in each circle from inside to outside in order by using cyclic command statements (Lu *et al.* 2013). Rod elements are generated by the following rules after node created. Let vertex be number 1. Applying loads on nodes whose number is less than the starting node number of the outermost circle and imposing displacement constraints on other nodes. Rod types, material properties, real constants, etc., are applied to analyze the structural internal force. Macro routines are compiled by using the parametric design language APDL in ANSYS (Chen and Liu 2009, Gong and Xie 2010).

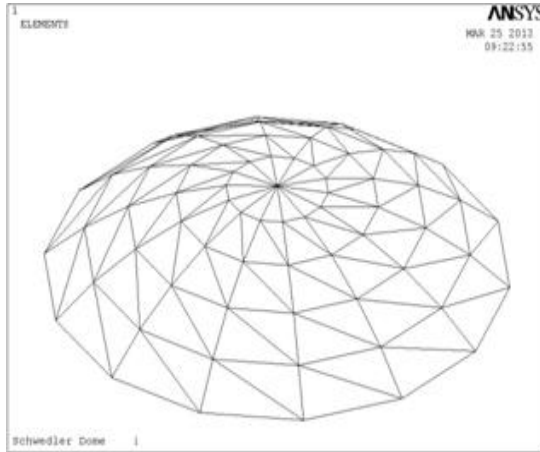
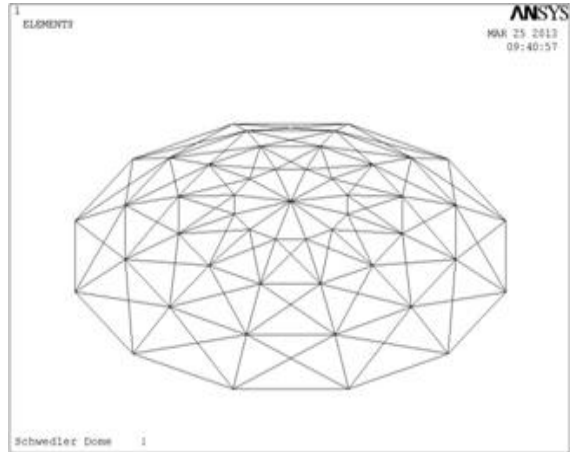
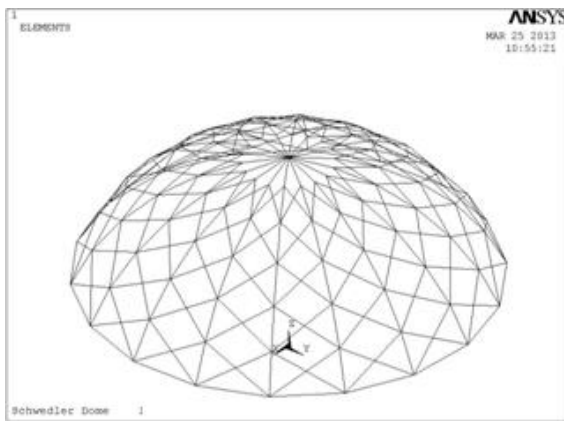
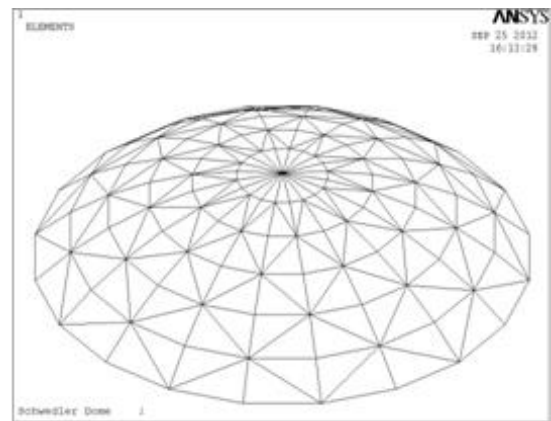
#### 3.1 Left diagonal rod-Schwedler spherical reticulated shell (Fig. 3)

Determine the numbers and coordinates of nodes: The node of the  $j$ -th at the  $i$ -th circle is numbered as  $1+Kn \times (i-1) + j$ , which coordinates are  $(R, (j-1) \times 360 / Kn, 90 - i \times Dpha)$ . Wherein  $i=3 \sim 12$ ,  $j=6 \sim 22$ .

Elements connection: a) The latitudinal elements at the  $i$ -th circle and  $j$ -th symmetric area are made by connecting the node  $1+Kn \times (i-1) + j$  and the node  $1+Kn \times (i-1) + j + 1$ . Elements at the last symmetric area of each circle are made by connecting the last node  $1+Kn \times i$  and the first node  $1+Kn \times (i-1) + 1$  of this circle. b) The radical elements at the  $j$ -th symmetric area between the  $i$ -th and  $(i+1)$ -th circles are made by connecting the node  $1+Kn \times (i-1) + j$  and the node  $1+Kn \times i + j$ . Elements between the apex and the first circle are made by connecting the node 1 and the node  $1+j$ . c) The diagonal elements at the  $j$ -th symmetric area between the  $i$ -th and  $(i+1)$ -th circles are made by connecting the node  $1+Kn \times (i-1) + j$  and the node  $1+Kn \times i + j + 1$ . Elements at the last symmetric area of each circle are made by connecting the node  $1+Kn \times i$  and the node  $1+Kn \times i + 1$ .

#### 3.2 Double slash rod-Schwedler spherical reticulated shell (Fig. 4)

Compared with left diagonal rod - Schwedler spherical reticulated shell, double slash rod have additional right diagonal rod. The right diagonal elements at the  $j$ -th symmetric area between the  $i$ -th and  $(i+1)$ -th circles are made by connecting the node  $1+Kn \times (i-1) + j + 1$  and the node  $1+Kn \times i + j$ .

Fig. 3 Left diagonal rod ( $Kn=14$ ,  $Nx=5$ )Fig. 4 Double slash rod ( $Kn=12$ ,  $Nx=4$ )Fig. 5 No latitudinal rod ( $Kn=18$ ,  $Nx=6$ )Fig. 6 Left and right rod ( $Kn=20$ ,  $Nx=6$ )

Elements at the last symmetric area of each circle are made by connecting the node  $1+Kn \times (i-1)+1$  and the node  $1+Kn \times (i+1)$ .

### 3.3 No latitudinal rod-Schwedler spherical reticulated shell (Fig. 5)

Compared with double slash rod - Schwedler spherical reticulated shell, no latitudinal rod only removes the latitudinal elements, but the outermost latitudinal rods are reserved.

### 3.4 Left and right rod-Schwedler spherical reticulated shell (Fig. 6)

The connection of latitudinal and radical elements is the same as left diagonal rod, the connection of diagonal elements as follows:

a) Odd-numbered circles: The diagonal elements at the  $j$ -th symmetric area between the  $i$ -th and  $(i+1)$ -th circles are made by connecting the node  $1+Kn \times (i-1) + j$  and the node  $1+Kn \times i + j + 1$ , the diagonal elements at the  $(j-1)$ -th symmetric area between the  $i$ -th and  $(i+1)$ -th circles are made by

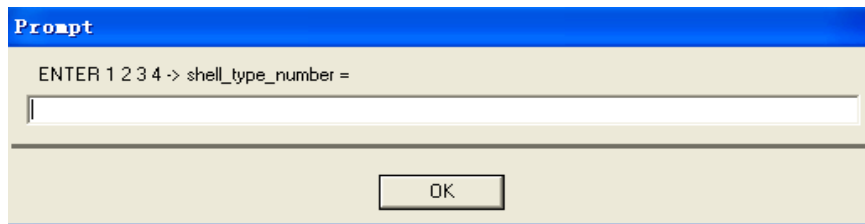


Fig. 7 Type selection window

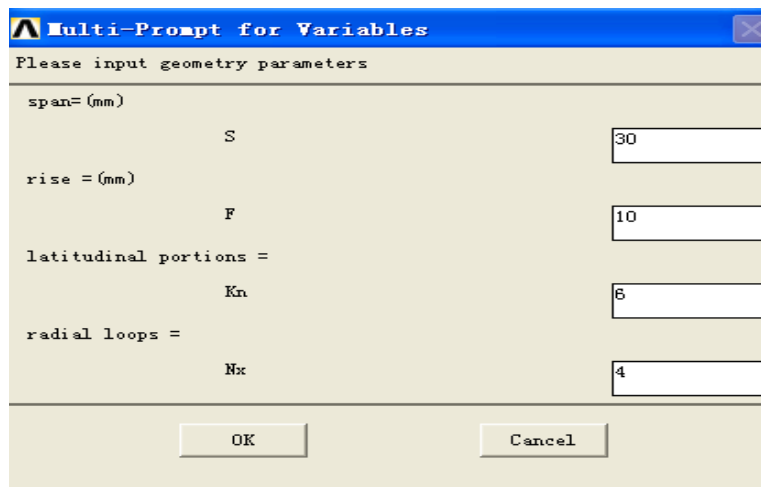


Fig. 8 Geometrical parameters window

connecting the node  $1+Kn \times (i-1) + j$  and the node  $Kn \times i + j$ , elements at the last symmetric area of each circle are made by connecting the node  $1+Kn \times (i-1) + 1$  and the node  $1+Kn \times (i+1)$ .

b) Even-numbered circles: The diagonal elements at the  $(j-1)$ -th symmetric area between the  $(i+1)$ -th and  $(i+2)$ -th circles are made by connecting the node  $Kn \times i + j$  and the node  $1+Kn \times (i+1) + j$ , the diagonal elements at the  $j$ -th symmetric area between the  $(i+1)$ -th and  $(i+2)$ -th circles are made by connecting the node  $1+Kn \times i + j + 1$  and the node  $1+Kn \times (i+1) + j$ , elements at the last symmetric area of each circle are made by connecting the node  $1+Kn \times (i+1)$  and the node  $1+Kn \times (i+1) + 1$ .

### 3.5 Preparation of entry interface

Through the compilation of type selection window, users can input program codes (1, 2, 3, 4) of four typical Schwedler spherical reticulated shells as needed, and enter the geometrical parameters interface. Then users can easily get the required models only by inputting parameters such as the shell span ( $S$ ), rise ( $F$ ), latitudinal portions ( $Kn$ ), radial loops ( $Nx$ ). Procedures are as follows:

Customizing programs of type selection window (Fig. 7)

FINISH

/PMACRO

/CLEAR, start

\*ASK, shell\_type\_number, 1 2 3 4

!1= Left diagonal rod; 2= Double slash rod; 3= No latitudinal rod; 4= Left and right rod;



## 5. The internal force analysis of four typical Schwedler spherical reticulated shells

The purpose of internal force analysis of Schwedler spherical reticulated shells is analyzing and calculating the displacements and stresses of the structures under loads and in the boundary conditions, and getting on structural design accordingly. The process of internal force analysis of Schwedler spherical reticulated shells is actually seeking rational shape, reasonable stress and distribution of stress, reasonable stiffness and distribution of stiffness continually.

Principles and methods of internal force analysis of Schwedler spherical reticulated shells are as follows (Shang and Qiu 2005):

Schwedler spherical reticulated shell as a used widely spatial structure, its analytical procedures are classic methods based on basic principles. The methods mainly include two categories: one is a method based on continuity assumption and the other based on discretization assumption.

The first method is imitative shell method. This method is to analyze and study the structures in accordance with the basic theory of elastic thin shells. Its purpose is to obtain the displacements and stresses of the structures and then convert into internal force of spherical reticulated shell structures. The second category is finite element method of truss structures. In other words, the grids constituted by rod members originally can disperse into individual element. And a rod member usually as a basic element when conducting internal force analysis.

As computer technology updates more quickly, finite element method of truss structures is usually adopted by Schwedler spherical reticulated shells at the time of internal force analysis. This method can be more flexible for linear (or nonlinear), static, dynamic and stability analysis of all types of reticulated shells. Internal force analysis of Schwedler spherical reticulated shells is carried out within the linear elastic range, and geometric nonlinearity of the material are generally not considered. This study make use of finite element analysis software (ANSYS) for internal force analysis of Schwedler spherical reticulated shells, meanwhile, beam elements of space are used as rod members, and assumed the nodes of spherical reticulated shells are ideal rigid joints.

In order to make the calculated results comparable, the relevant parameters are the same. Constraint conditions of the outermost nodes of Schwedler spherical reticulated shells are simply supported. Hot rolled seamless steel pipe (calculated by YB 231-70) is adopted as rod elements of Schwedler spherical reticulated shells. The model information of four typical Schwedler spherical reticulated shells is shown in Table 1. Stress and displacement contours are shown in Fig. 10 (such left diagonal rod - Schwedler spherical reticulated shell as an example). The internal force analysis results of four typical Schwedler spherical reticulated shells are shown in Table 2.

Table 2 shows that:

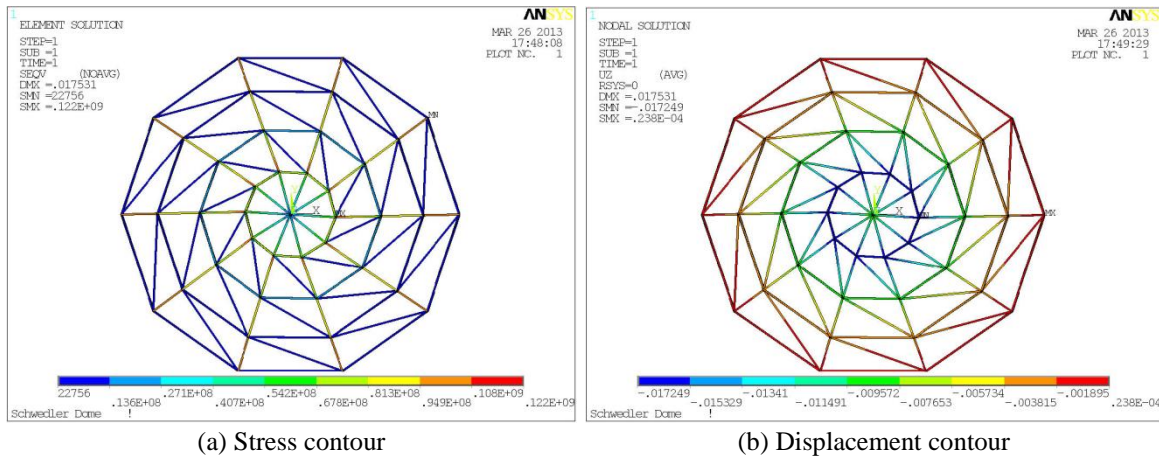
(1) Among the four typical Schwedler spherical reticulated shells, the maximum stress and displacement of double slash rod is the smallest, followed by left and right rod, then left diagonal rod, and no latitudinal rod is the biggest.

Table 1 The model information of four typical Schwedler spherical reticulated shells

Type	Left diagonal rod, Double slash rod, No latitudinal rod, Left and right rod		
Span (Rise to span ratio )	30 m (1/5), 60 m (1/6), 90 m (1/5)		
Steel density	7800 kg/m <sup>3</sup>	Elastic modulus	2.06 × 10 <sup>5</sup> Mpa
Poisson ratio	0.3	Yield strength	2.15 × 10 <sup>8</sup> N/m <sup>2</sup>
Even load	2.35 kN/m <sup>2</sup>		

Table 2 The internal force analysis results of four typical Schwedler spherical reticulated shells

Span (m)	Type	Rise to span ratio	$Kn$	$Nx$	The maximum Stress (Mpa)	The maximum displacement (mm)
30	Left diagonal rod	1/5	10	4	122	17.249
	Double slash rod	1/5	10	4	99	14.052
	No latitudinal rod	1/5	10	4	167	25.217
	Left and right rod	1/5	10	4	121	16.963
60	Left diagonal rod	1/6	14	5	152	46.370
	Double slash rod	1/6	14	5	118	38.388
	No latitudinal rod	1/6	14	5	198	62.841
	Left and right rod	1/6	14	5	150	45.498
90	Left diagonal rod	1/5	16	6	183	54.121
	Double slash rod	1/5	16	6	132	45.635
	No latitudinal rod	1/5	16	6	201	75.512
	Left and right rod	1/5	16	6	179	52.899

Fig. 10 Left diagonal rod - Schwedler spherical reticulated shell ( $S=30$ ,  $F=6$ ,  $Kn=10$ ,  $Nx=4$ )

(2) The maximum stresses and displacements all appeared at vicinity of the vertex and the first circle latitudinal rods. Due to the structures without latitudinal rods, no latitudinal rod has poor mechanical properties. In contrast, double slash rod has better mechanical behavior because of the dense grids. The maximum stresses and displacements have little difference between left and right rod and left diagonal rod, and both of them have reasonable force distribution.

## 6. Shape optimization programming

The principles of shape optimization, from Sections 6.1 to 6.3, are the same as our previous study (Wu *et al.* 2015). However, the optimized objects are different, thus the corresponding conclusions are also different.

### 6.1 Mathematical models of shape optimization

#### 6.1.1 Design variables

The cross-sectional area of the rod member  $A_i$  ( $i=1, 2, \dots, m$ ),

The volume of the node  $V_j$  ( $j=1, 2, \dots, n$ ).

#### 6.1.2 The objective function

The total weight of shell structures

$$\min W = \sum_{i=1}^m \rho_i l_i A_i + \sum_{j=1}^n \rho_j V_j \quad (3)$$

where  $m$  is the number of rod elements;  $n$  is the number of nodes;  $A_i$  is cross-sectional area of the  $i$ -th rod element, ( $m^2$ );  $\rho_i, \rho_j$  are density of steel of rod elements and nodes respectively, ( $kg/m^3$ );  $l_i$  is geometry length of the  $i$ -th rod element, (m);  $V_j$  is volume of the  $j$ -th ball node, ( $m^3$ ); The volume of hollow ball,  $V_j = \pi d^2 t$ ,  $t$  is the wall thickness of welded hollow spherical joints, (mm).

#### 6.1.3 Constraint conditions

1) Deflection Constraints

$$\delta_{\max} \leq [\delta] \quad (4)$$

where  $\delta_{\max}$  is the maximum calculated deflection,  $[\delta]$  is the allowable deflection.

2) Strength constraints of the rods:

Pull rod

$$\sigma_i = \frac{N_i}{A_i} \leq [\sigma] \quad (5)$$

where  $N_i$  is axial pull of the  $i$ -th pull rod, ( $N$ );  $[\sigma]$  is the design strength.

Pressure rod

$$\sigma_i = \frac{N_i}{\varphi_i A_i} \leq [\sigma] \quad (6)$$

where  $N_i$  is axial pressure of the  $i$ -th pressure rod, ( $N$ );  $\varphi_i$  is stability factor of the  $i$ -th pressure rod.

3) Slenderness ratio of the rods

$$\lambda_i = \frac{l_{0i}}{r_i} \leq [\lambda] \quad (7)$$

where  $l_{0i}$  is geometry length of the  $i$ -th rod element, (m);  $r_i$  is cross-sectional radius of gyration of the  $i$ -th rod element, (m);  $\lambda_i$  is slenderness ratio of the  $i$ -th rod element,  $[\lambda]$  is the allowable slenderness ratio.

4) Upper and lower constraints of cross-section of the rods:

$$A_i \in \{A\} \quad (8)$$

$$V_j \in \{V\} \quad (9)$$

$$S_k \in \{S\} \quad (10)$$

where  $\{A\}$  is a variable discrete set of cross-sectional dimensions of the rods;  $\{V\}$  is a variable discrete set of volume of the nodes;  $\{S\}$  is a variable discrete set of structural geometry.

5) Constraints of the nodes:

Welded hollow spherical

$$D_{\min} \geq \frac{d_1 + d_2 + 2\alpha_n}{\theta} \quad (11)$$

where  $d_1, d_2$  is the outer diameter of two adjacent rods, (mm);  $\theta$  is the angle between two adjacent rods, (rad);  $\alpha_n$  is clear distance between adjacent rods in the spherical surface.

## 6.2 Cross-sectional optimization

In the present study, the designed algorithms of two-stage cross-sectional optimization are adopted, which is based on discrete variables. The first stage makes use of a one-dimensional search algorithm to process local constraints, and the second stage takes advantage of a relative difference quotient algorithm to handle whole constraints (Deng and Dong 1999). The mathematical models of cross-sectional optimization are as follows (Lu *et al.* 2013, Wu *et al.* 2015, Sun *et al.* 2002)

$$\begin{aligned}
 &P_1 \quad \text{Seeking } A \\
 \min W &= \sum_{i=1}^m \rho_i l_i(S) A_i + \sum_{j=1}^n \rho_j V_j \\
 \text{s.t.} \quad &\sigma_{wi} \leq [\sigma] \\
 &\lambda_i \leq [\lambda] \\
 &x_i \in S_i
 \end{aligned} \quad (12)$$

## 6.3 Shape optimization

The mathematical models (Lu *et al.* 2013, Wu *et al.* 2015, Sun *et al.* 2002) of shape optimization

$$\begin{aligned}
 &P_2 \quad \text{Seeking } kn, nx \\
 \min W &= \sum_{i=1}^m \rho_i l_i(kn, nx) A_i + \sum_{j=1}^n \rho_j V_j \\
 \text{s.t.} \quad &\delta_{\max} \leq [\delta]
 \end{aligned} \quad (13)$$

Given the range of  $Kn$  and  $Nx$ , searching combination of  $Kn$  and  $Nx$ , in order to minimize total steel consumption of spherical reticulated shells.

#### 6.4 Programming

For Schwedler spherical reticulated shells, the number of rod elements and nodes are the main factors affecting the total weight of the structures. This study takes the total steel consumption of reticulated shells (including the weight of rods and nodes) as objective function. Meanwhile,  $Kn$  and  $Nx$  are taken as design variables (Lu *et al.* 2012, Wu *et al.* 2015). A shape optimization program is compiled in FORTRAN environment. The most important feature of the program is that it can drive large-scale finite element analysis software ANSYS to re-analysis and re-checking of internal forces constantly in the background, so that modeling, solving and optimized design can be achieved. Moreover, Modular, structural design ideas (Deng and Dong 1999, Xu *et al.* 2006) are adopted, so that the programs can be modified, extended, and transplanted in follow-up works.

##### (1) Steps of an algorithm

Firstly, an initial cross-sectional area of rod element  $A^{(0)}$  is given based on design experience and estimation. The design variable cross-sectional area of rod elements in this study should meet the following requirements

$$\begin{aligned} A^{(0)} &= \left( A_1^{(0)}, A_2^{(0)}, \dots, A_j^{(0)}, \dots, A_n^{(0)} \right)^T \\ A^{(k)} &= \left( A_1^{(k)}, A_2^{(k)}, \dots, A_j^{(k)}, \dots, A_n^{(k)} \right)^T \\ A^{(k)} &\geq A^{(0)} \end{aligned} \quad (14)$$

Wherein,  $A^{(k)}$  represents the cross-sectional area of rod elements after the  $k$ -th iteration. Secondly, the stress ratio of rod elements is calculated.

$$U_i^{(k)} = \frac{|N_i^{(k)}|}{e_w A_i^{(k)}} + \frac{|M_i^{(k)}|}{e_w W_i^{(k)}} \times 0.9 \quad (15)$$

Wherein,  $N_i^{(k)}$  is axial pressure of rod elements after the  $k$ -th iteration,  $M_i^{(k)}$  is the maximum bending moment in the range of rod elements after the  $k$ -th iteration,  $A_i^{(k)}$  is the cross-sectional area of rod elements after the  $k$ -th iteration,  $W_i^{(k)}$  is the section modulus of rod elements after the  $k$ -th iteration,  $e_w$  is the allowable stress.

Then, the common iterative formula is formulated.

$$A_i^{(k+1)} = U_i^{(k)} A_i^{(k)} \quad (16)$$

$U_i^{(k)}$  is the stress ration of the  $i$ -th rod element during the  $k$ -th iteration.

##### (2) Convergence criterion

During the global optimization,

$$\left| 1 - \frac{W^{(k+1)}}{W^{(k)}} \right| \leq \varepsilon_2 \quad (17)$$

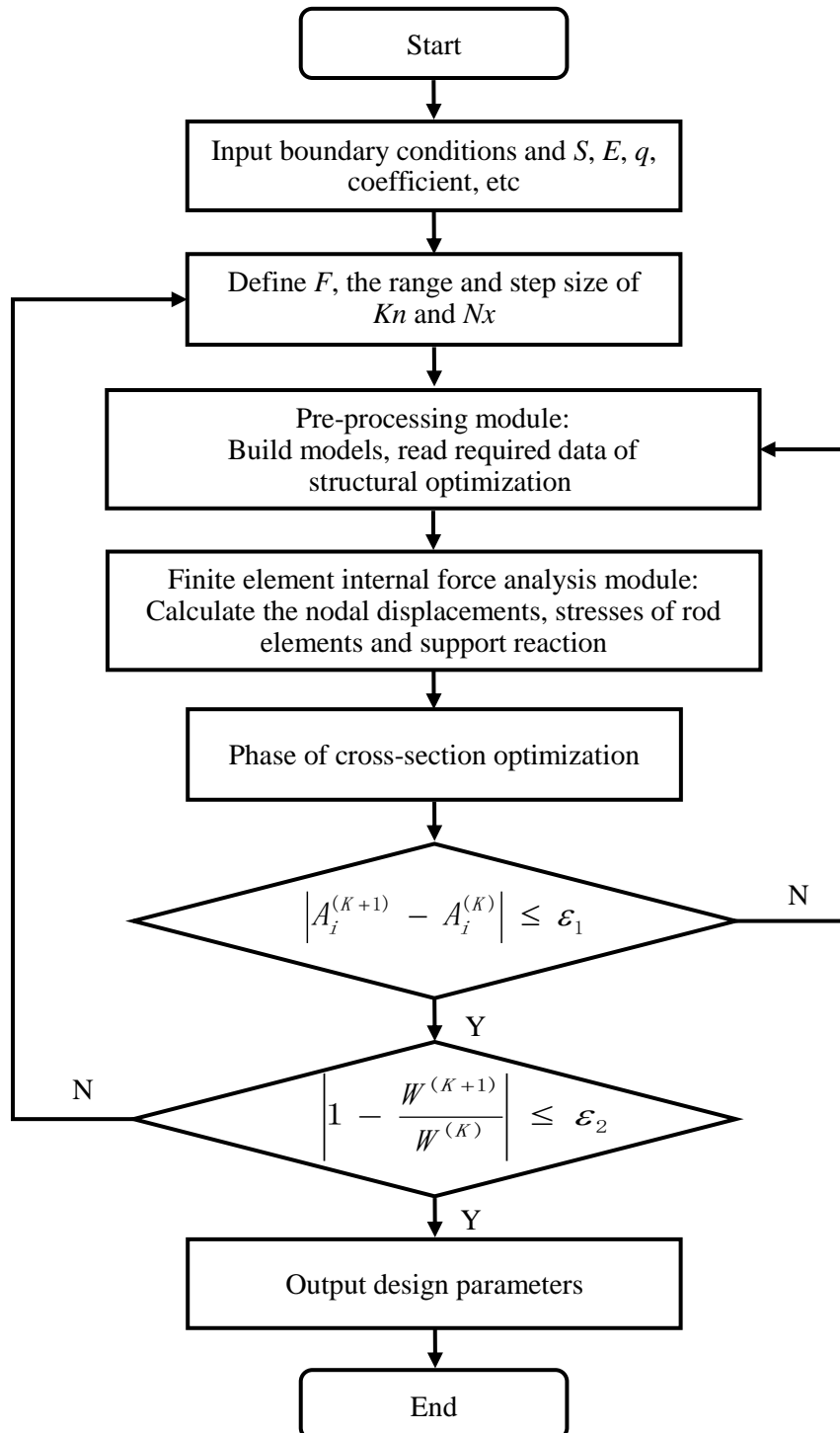


Fig. 11 Shape optimization flowchart of Schwedler spherical reticulated shells

Wherein,  $W^{(k+1)}$ ,  $W^{(k)}$  represent the total weight of shell structures after  $(k+1)$ -th and  $k$ -th iterations, respectively.  $\varepsilon_2$  is a positive decimal value.

During the local optimization

$$|A_i^{(k+1)} - A_i^{(k)}| \leq \varepsilon_1 \tag{18}$$

Wherein,  $A_i^{(k+1)}$ ,  $A_i^{(k)}$  represent the cross-sectional area of the  $i$ -th rod element after the  $(k+1)$ -th and  $k$ -th iterations, respectively.  $\varepsilon_1$  is a positive decimal value.

(3) Optimization methods

Start with the global optimization (Xu *et al.* 2006), then, the local optimization, followed by the global optimization, this cyclic process is adopted in the present study. The cross-sectional area of rod elements and the volume of nodes are used as primary design variables in cross-sectional optimization (local optimization), while  $Kn$  and  $Nx$  are taken as primary design variables in shape optimization (global optimization). Meanwhile, the method of alternating primary and secondary design variables continually is used, which makes original coupling relations of the design variables simplified, moreover, the interplay between them is also considered, which makes the whole and local coordinate. Make sure the whole optimal point is based on the local optimal point. The cycle is kept going until it satisfies all the constraints. Different convergence conditions are adopted at different stages, which make the program have extensive applicability.

The range of  $Kn$  and  $Nx$  is defined beforehand in optimization program based on theoretical and practical problems. Under the certain rise to span ratio, from one side, if the  $Kn$  and  $Nx$  are too large, the grid of the shells will be too thick, especially the radical rod elements at the position of the vertex, if the  $Kn$  is too large, welded-sphere joints must be big enough to ensure these certain holes, which makes it difficult to construct. From the other side, if the  $Kn$  and  $Nx$  are too small, the grid of the shells will be too thin, which leads to unreasonable stress problems. Therefore, as for spherical reticulated shells of different span and height, the range of  $Kn$  and  $Nx$  is selected appropriately based on theoretical and practical experiences in optimization program.

In order to present the process of shape optimization intuitively, Fig. 11 gives the flowchart of Schwedler spherical reticulated shells (Wu *et al.* 2015).

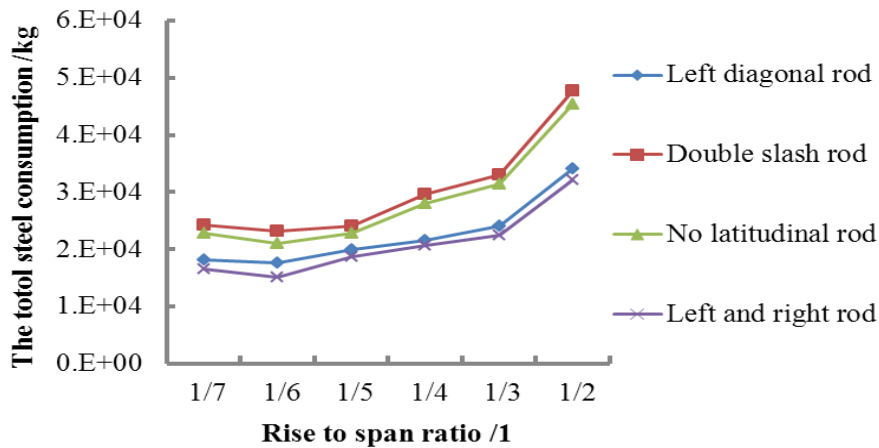


Fig. 12 The total steel consumption of four typical Schwedler spherical reticulated shells when span is 30 m

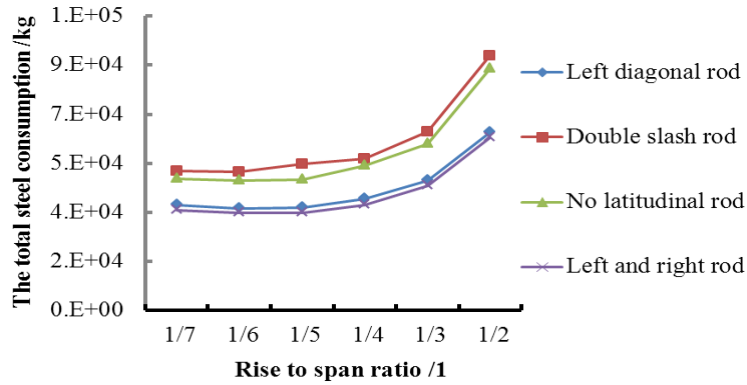


Fig. 13 The total steel consumption of four typical Schwedler spherical reticulated shells when span is 40 m

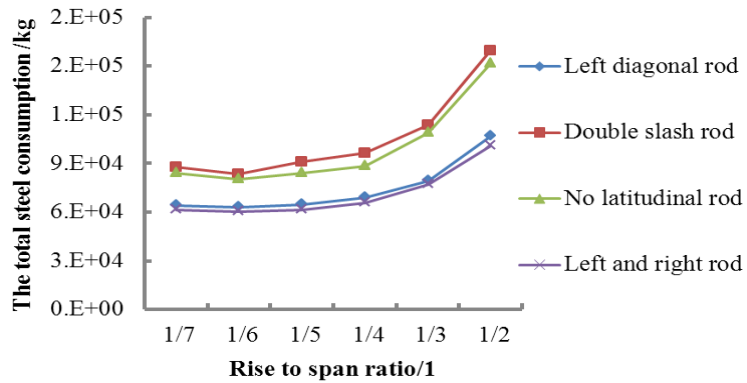


Fig. 14 The total steel consumption of four typical Schwedler spherical reticulated shells when span is 50 m

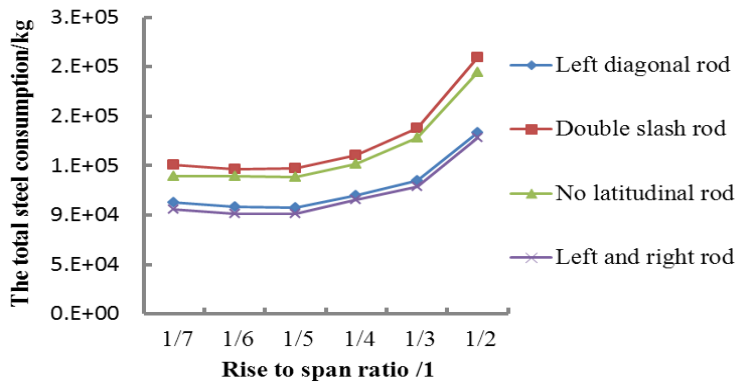


Fig. 15 The total steel consumption of four typical Schwedler spherical reticulated shells when span is 60 m

### 7. Shape optimization results and discussion

Under the same  $S$ ,  $Kn$  and  $Nx$ , different rise to span ratio, the total steel consumption of four typical Schwedler spherical reticulated shells after optimization are shown in Figs. 12-17.

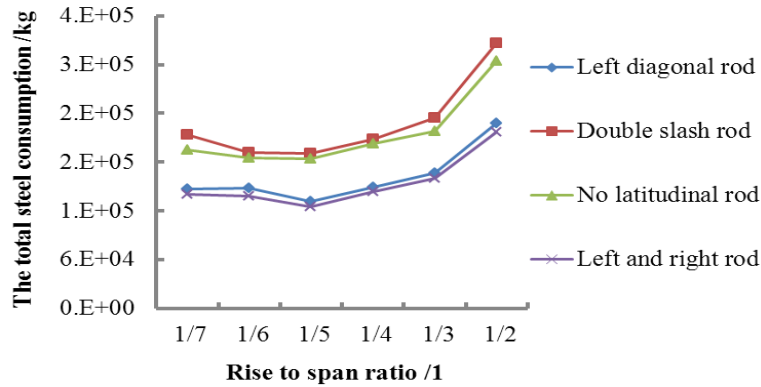


Fig. 16 The total steel consumption of four typical Schwedler spherical reticulated shells when span is 70 m

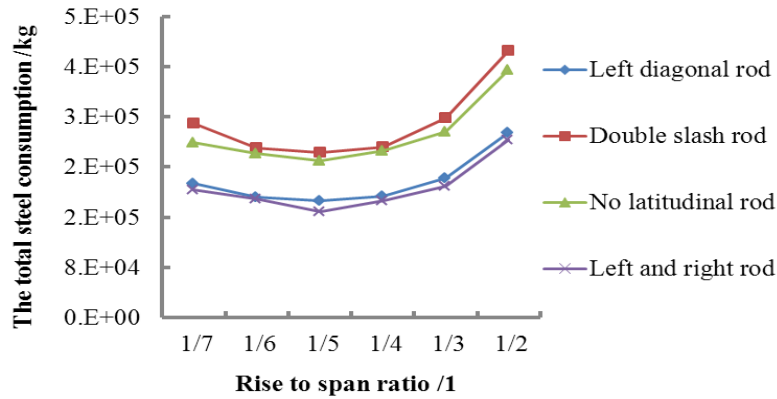


Fig. 17 The total steel consumption of four typical Schwedler spherical reticulated shells when span is 80 m

(1) When the span is 30 m, it can be seen clearly from Fig. 12: The total weight of double slash rod after shape optimization is the maximum, followed by no latitudinal rod, then left diagonal rod, and the total weight of left and right rod after shape optimization is the lightest. It also shows, the total weight of four typical Schwedler spherical reticulated shells is minimal when the rise to span ratio is 1/6. The result is obtained from the optimizer, i.e., when the rise to span ratio of the structures is 1/6, the selected cross-sectional area of rod elements and volume of nodes are relatively smaller on the premise of satisfying all the constraint conditions. From the aspect of internal force analysis, in such cases, the stress and displacement are both smaller, and the structures have reasonable force. In this case, the difference of total weight between double slash rod and no latitudinal rod is  $2 \times 10^3$  kg, and the difference of total weight between left diagonal rod and left and right rod is close to  $2 \times 10^3$  kg, meanwhile, the difference between the maximum and minimum is  $8 \times 10^3$  kg.

(2) Similarly, when the span is 40 m (Fig. 13), the results are basically consistent with the analysis of Fig. 12. While the rise to span ratio is 1/6, the difference of total weight between double slash rod and no latitudinal rod is  $3 \times 10^3$  kg, and the difference of total weight between left diagonal rod and left and right rod is  $2 \times 10^3$  kg, meanwhile, the difference between the maximum and minimum is  $1.5 \times 10^4$  kg, which has nearly doubled than the difference when the span is 30 m.

(3) When the span is 50 m and rise to span ratio is 1/6 (Fig. 14), the difference of total weight between double slash rod and no latitudinal rod is  $3 \times 10^3$  kg, and the difference of total weight between left diagonal rod and left and right rod is  $2.3 \times 10^3$  kg, meanwhile, the difference between the maximum and minimum is  $2.3 \times 10^4$  kg, which has increased two times than the difference when the span is 30 m.

(4) When the span is 60 m and rise to span ratio is 1/6 (Fig. 15), the difference of total weight between double slash rod and no latitudinal rod is  $6 \times 10^3$  kg, and the difference of total weight between left diagonal rod and left and right rod is close to  $6 \times 10^3$  kg, meanwhile, the difference between the maximum and minimum is  $4 \times 10^4$  kg, which has increased four times than the difference when the span is 30 m.

(5) When the span is 70 m, it can be seen clearly from Fig. 16: The total weight of double slash rod after shape optimization is the maximum, followed by no latitudinal rod, then left diagonal rod, and the total weight of left and right rod after shape optimization is the lightest. It also shows, the total weight of four typical Schwedler spherical reticulated shells is minimal when the rise to span ratio is 1/5. In this case, the difference of total weight between double slash rod and no latitudinal rod is  $7 \times 10^3$  kg, and the difference of total weight between left diagonal rod and left and right rod is  $7 \times 10^3$  kg, meanwhile, the difference between the maximum and minimum is  $6.5 \times 10^4$  kg, which has increased seven times than the difference when the span is 30 m.

(6) Likewise, when the span is 80 m (Fig. 17), the results are basically consistent with the analysis of Fig. 16. While the rise to span ratio is 1/5, the difference of total weight between double slash rod and no latitudinal rod is  $1.3 \times 10^4$  kg, and the difference of total weight between left diagonal rod and left and right rod is  $1.6 \times 10^4$  kg, meanwhile, the difference between the maximum and minimum is  $9 \times 10^4$  kg, which has increased ten times than the difference when the span is 30 m.

(7) Overall, when the span is less than 60 meters, the difference of total weight of four typical Schwedler spherical reticulated shells is small. Otherwise, the total weight increased rapidly. When the span is 60 meters, the total weight of double slash rod and no latitudinal rod is much greater than left and right rod and left diagonal rod. And as the span increases, the difference is also growing. When the span is 80 meters, the maximum difference has increased by nearly tenfold more.

(8) Under the same span and rise to span ratio, after shape optimization, the total weight of double slash rod is the maximum. That is because the grids of double slash rod are denser and the number of rod elements is larger, thereby increasing its weight.

(9) Under the certain span, the total weight of four typical Schwedler spherical reticulated shells changes with the changes of rise to span ratio. When the rise to span ratio is between 1/6 to 1/5, the figure is the lightest.

(10) In a word, when the span is between 30 to 80 meters, the total weight of left and right rod after shape optimization is the minimum, followed by left diagonal rod, and the total weight of no latitudinal rod and double slash rod after shape optimization is larger. Thus, left and right rod-Swedler spherical reticulated shell can be used for large, medium and small-span structures from the viewpoint of economic aspect, which has broad scope of application.

## 8. Conclusions

Parametric modeling and shape optimization of four typical Schwedler spherical reticulated

shells are achieved in the present study.

Generation methods of nodes and the corresponding connection methods of rod elements are proposed. Modeling programs are compiled by adopting the APDL. The internal forces of four typical Schwedler spherical reticulated shells are analyzed. A shape optimization method based on the two-stage algorithm is presented, and the corresponding optimization program is compiled in FORTRAN environment. Shape optimization is conducted by considering the objective function of the minimum total steel consumption, global and locality constraints. The shape optimization of four typical Schwedler spherical reticulated shells is carried out with the span of 30 m~80 m and rise to span ratio of 1/7~1/2. Compared with the shape optimization results, the variation rules of total steel consumption along with the span and rise to span ratio are discussed. The results show that:

- From the viewpoint of internal force analysis and shape optimization, left and right rod-Swedler spherical reticulated shell is the most optimized and should be preferentially adopted in structural engineering. It can be widely used in large, medium and small-span structures.
- The left diagonal rod-Swedler spherical reticulated shell is second only to left and right rod regarding the mechanical behavior and optimized results. It can be applied to medium and small-span structures.
- After internal force analysis, the stress and displacement of double slash rod-Swedler spherical reticulated shell is minimal. However, the total weight of the optimized structure is the largest. Thus, this type can be used in large-span structures as far as possible.
- Because the stress and displacement under the loads of no latitudinal rod-Swedler reticulated shell is the largest. In addition, the total weight of the optimized structure is the second largest. Thus, this spherical reticulated shell should not be adopted generally in engineering.

## Acknowledgments

This study was financially supported by the National Basic Research Program of China (973 Program, No.: 2013CB036000), the National Natural Science Foundation of China (Grant No.: 51479106, 41302225, 51509147), the promotive research fund for excellent young and middle-aged scientists of Shandong Province (Grant No.: 2014GN028) and the China Postdoctoral Science Foundation (Grant No.: 2014M551908).

## References

- Chai, S. and Sun, H.C. (1996), "A two-level delimitative and combinatorial algorithm for a kind of (0, 1, 2) programming", *J. Dalian Univ. Tech.*, **36**(3), 258-263.
- Chiu, M.C. (2010), "Shape optimization of multi-chamber mufflers with plug-inlet tube on a venting process by genetic algorithms", *Appl. Acoust.*, **71**(6), 495-505.
- Deng, H. and Dong, S.L. (1999), "Shape optimization of spatial reticulated shell structures", *J. Zhejiang Univ. (Eng. Sci.)*, **33**(4), 371-375.
- Dong, S.L. and Yao, J. (2003), "Future and prospects of reticulated shells", *Spatial Struct.*, **9**(1), 31-34.
- Dietl, J.M. and Garcia, E. (2010), "Beam shape optimization for power harvesting", *J. Intel. Mater. Syst. Struct.*, doi: 10.1177/1045389X10365094.
- Durgun, İ. and Yildiz, A.R. (2012), "Structural design optimization of vehicle components using cuckoo

- search algorithm”, *Mater. Test.*, **54**(3), 185-188.
- Emmanuel Nicholas, P., Padmanaban, K.P. and Vasudevan, D. (2014), “Buckling optimization of laminated composite plate with elliptical cutout using ANN and GA”, *Struct. Eng. Mech.*, **52**(4), 815-827.
- Fraternali, F., Marino, A., Sayed, T. E. and Cioppa, A.D. (2011), “On the structural shape optimization through variational methods and evolutionary algorithms”, *Mech. Adv. Mater. Struct.*, **18**(4), 225-243.
- Gholizadeh, S and Barzegar, A. (2013), “Shape optimization of structures for frequency constraints by sequential harmony search algorithm”, *Eng. Optim.*, **45**(6), 627-646.
- Jenkins, W.M. (1991), “Towards structural optimization via the genetic algorithm”, *Comput. Struct.*, **40**(5), 1321-1327.
- Jenkins, W.M. (1991), “Structural optimization with the genetic algorithm”, *Struct. Eng.*, **69**(24), 418-422.
- Jenkins, W.M. (1997), “On the application of natural algorithms to structural design optimization”, *Eng. Struct.*, **19**(4), 302-308.
- Kaveh, A. and Ahmadi, B. (2014), “Sizing, geometry and topology optimization of trusses using force method and supervised charged system search”, *Struct. Eng. Mech.*, **50**(3), 365-382.
- Kaveh, A. and Zolghadr, A. (2014), “A new PSRO algorithm for frequency constraint truss shape and size optimization”, *Struct. Eng. Mech.*, **52**(3), 445-468.
- Lipson, S.L. and Gwin, L.B. (1977), “Discrete sizing of trusses for optimal geometry”, *J. Struct. Div.*, **103**(5), 1031-1046.
- Lu, X.Y., Zhao, X.W. and Huang, L.L. (2012), “Shape optimizing design of kiewiti spherical reticulated shell”, *Adv. Mater. Res.*, **424**, 324-329.
- Luo, Z., Zhang, N., Gao, W. and Ma, H. (2012), “Structural shape and topology optimization using a meshless Galerkin level set method”, *Int. J. Numer. Meth. Eng.*, **90**(3), 369-389.
- Pedersen, N.L. (2010), “Improving bending stress in spur gears using asymmetric gears and shape optimization”, *Mech. Machine Theor.*, **45**(11), 1707-1720.
- Qian, X. (2010), “Full analytical sensitivities in NURBS based isogeometric shape optimization”, *Comput. Meth. Appl. Mech. Eng.*, **199**(29), 2059-2071.
- Rajan, S.D. (1995), “Sizing, shape, and topology design optimization of trusses using genetic algorithm”, *J. Struct. Eng.*, **121**(10), 1480-1487.
- Rahami, H., Kaveh, A. and Gholipour, Y. (2008), “Sizing, geometry and topology optimization of trusses via force method and genetic algorithm”, *Eng. Struct.*, **30**(9), 2360-2369.
- Svanberg, K. (1987), “The method of moving asymptotes-a new method for structural optimization”, *Int. J. Numer. Meth. Eng.*, **24**(2), 359-373.
- Sun, H.C., Wang, Y.F. and Huang, J.F. (1995), “Shape optimization designs of trusses with discrete variables”, *J. Dalian Univ. Tech.*, **35**(1), 10-16.
- Saka, M.P. and Kameshki, E.S. (1998), “Optimum design of nonlinear elastic framed domes”, *Adv. Eng. Softw.*, **29**(7), 519-528.
- Salajegheh, E. and Vanderplaats, G.N. (1993), “Optimum design of trusses with discrete sizing and shape variables”, *Struct. Optim.*, **6**(2), 79-85.
- Salajegheh, E. (2000), “Optimum design of structures with high-quality approximation of frequency constraints”, *Adv. Eng. Softw.*, **31**(6), 381-384.
- Vyzantiadou, M.A., Avdelas, A.V. and Zafiroopoulos, S. (2007), “The application of fractal geometry to the design of grid or reticulated shell structures”, *Comput. Aid. Des.*, **39**(1), 51-59.
- Yildiz, A.R. (2013), “Comparison of evolutionary-based optimization algorithms for structural design optimization”, *Eng. Appl. Artif. Intel.*, **26**(1), 327-333.
- Wu, W., Petrini, L., Gastaldi, D., Villa, T., Vedani, M., Lesma, E. and Migliavacca, F. (2010), “Finite element shape optimization for biodegradable magnesium alloy stents”, *Ann. Biomed. Eng.*, **38**(9), 2829-2840.
- Wu, J., Lu, X.Y., Li, S.C., Zhang, D.L., Xu, Z.H., Li, L.P. and Xue, Y.G. (2015), “Shape optimization for partial double-layer spherical reticulated shells of pyramidal system”, *Struct. Eng. Mech.*, **55**(3), 555-581.
- Xu, J., Yang, S.S. and Diao, Y.S. (2006), “Optimized design of single - layer reticulated shell”, *Spat. Struct.*, **12**(3), 35-37.

- Xia, Q., Shi, T., Liu, S. and Wang, M.Y. (2012), "A level set solution to the stress-based structural shape and topology optimization", *Comput. Struct.*, **90**, 55-64.
- Yas, M.H., Shakeri, M. and Ghasemi-Gol, M. (2007), "Two-objective stacking sequence optimization of a cylindrical shell using genetic algorithm", *Scientia Iranica*, **14**(5), 499-506.
- Chen, Z.H. and Liu, H.B. (2009), *APDL Parametric Calculation and Analysis*, China Water Power Press, Beijing, China.
- Gong, S.G. and Xie, G.L. (2010), *ANSYS Parametric Programming and Command Manual*, China Machine Press Beijing, China.
- Lu, X.Y., Zhao, X.W. and Chen, S.Y. (2013), *The Optimization of Reticulated Shell Structures Based On Discrete Variables*, Building Industry Press, Beijing, China.
- Sun, H.C., Chai, S. and Wang, Y.F. (2002), *Structural Optimization with Discrete Variables*, Dalian University of Technology Press, Dalian, China.
- Shen, Z.Y. and Chen, Y.J. (1996), *Grid and Lattice Shell*, Tongji University Press, Shanghai, China.
- Shang, X.J. and Qiu, F. (2005), *ANSYS Structural Finite Element Senior Analysis Method and Sample Applications*, China Water Power Press, Beijing, China.
- Wu, J. (2013), "Parametric modeling and shape optimization of four typical schwedler reticulated shells", Mater Dissertation, Shandong Jianzhu University, Jinan.